Spatial and Transient Characteristics of Reflector Temperature Feedback in a BeO-Reflected Fast-Spectrum Molten Salt Reactor

Seong Jun Yoon[a*], Yubin Go[a], Sung-Kyun Zee[a], Tongkyu Park[a], Jae Uk Seo[a]
[a] *FNC Technology, Heungdeok IT Valley Bldg. 20F, 12, Heungdeok 1-ro, Giheung-gu, Yongin-si, Gyeonggi-do, 16954, Republic of Korea*
[*] *Corresponding author: sjyoon@fnctech.com*

Keywords : Micro Reactor, Small Modular Reactor, Molten Salt Fast Reactor, Reflector Temperature Coefficient

1. Introduction

Microreactors, including molten salt reactors (MSRs), have attracted increasing attention for applications requiring compactness, transportability, and inherent safety. For fast-spectrum MSRs, minimizing neutron leakage is particularly important for achieving a compact core. Beryllium oxide (BeO) is an attractive reflector material because of its favorable neutronic and high-temperature properties, enabling a significant reduction in core size.

However, the incorporation of BeO presents multiple design challenges, such as power concentration near the core–reflector interface, which affects local flow and thermal-hydraulic design, as well as lithium and tritium production and irradiation-induced swelling. In addition, the examined BeO-reflected fast-spectrum MSR exhibits a positive reflector temperature coefficient (RTC). This positive feedback can partially offset the negative fuel temperature and density feedbacks and therefore requires careful consideration in transient and inherent safety analyses.

The actual RTC during a transient may differ from that deduced from a static temperature perturbation because of reflector thermal inertia and the spatial dependence of reactivity contributions. In particular, the positive RTC may develop more slowly than the negative fuel feedbacks, affecting the transient reactivity balance. In this study, the BeO reflector is divided into multiple radial regions to assess the spatial sensitivity of the RTC. A reduced-order transient model that couples point kinetics with fuel and reflector thermal feedbacks is then applied to explore the spatially dependent and delayed development of the RTC under transient conditions.

2. Calculation Models

Previous studies have investigated delayed-neutron precursor transport and effective delayed-neutron fractions in circulating-fuel MSRs [3], as well as coupled neutronic–thermal-hydraulic effects in MSFRs with moderating reflectors [4]. The reduced-order transient model employed in the present study was developed to represent these relevant physical effects in a simplified form. A reduced-order transient model was formulated in perturbation form by coupling point kinetics, circulating delayed-neutron precursor transport, and one-dimensional fuel/reflector energy balances. OpenMC pre-calculations provide the kinetics and spatial feedback inputs, while the transient model solves only deviations from a prescribed reference state. Figure 1 summarizes the calculation sequence.

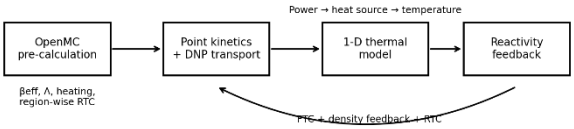


Fig. 1. Reduced-order multi-physics analysis framework.

The normalized power n and the core/loop precursor concentrations Cc,i and Cl,i are governed by

$$\frac{dn}{dt} = \frac{\rho - \beta_{eff}}{\Lambda} n + \sum_{i=1}^{G} \lambda_i C_{c,i} \quad (1)$$

$$\frac{dC_{c,i}}{dt} = \frac{\beta_i}{\Lambda} n - \lambda_i C_{c,i} - \frac{C_{c,i}}{\tau_c} + \frac{C_{l,i}}{\tau_l} \quad (2a)$$

$$\frac{dC_{l,i}}{dt} = \frac{C_{c,i}}{\tau_c} - \lambda_i C_{l,i} - \frac{C_{l,i}}{\tau_l} \quad (2b)$$

The total reactivity is decomposed as

$$\rho = \rho_{base} + \rho_{ext} + \alpha_f \Delta T_f + \alpha_\rho (\rho_{f,0} - \rho_f) + \sum_{i=1}^{6} \alpha_{RTC,i} \Delta T_{R,i} \quad (3)$$

The thermal model is written in delta form. For the fuel and the first reflector node, for example,

$$M_f c_{p,f} \frac{d\Delta T_f}{dt} = f_f \Delta P - H_{fR}(\Delta T_f - \Delta T_{R,1}) - H_{fs} \Delta T_f \quad (4a)$$

$$M_{R,1} c_{p,R} \frac{d\Delta T_{R,1}}{dt} = f_{R,1} \Delta P + H_{fR}(\Delta T_f - \Delta T_{R,1}) + K_{R,1}(\Delta T_{R,2} - \Delta T_{R,1}) \quad (4b)$$

Analogous radial conduction balances are applied to the remaining reflector nodes, with heat removal from the outermost node. Here $\Delta P = P - P0$ and $f_f = 1 - \Sigma f_{R,i} = 0.9587$. The initial conditions are $n(0) = 1$ and $\Delta T_f(0) = \Delta T_{R,i}(0) = 0$, with precursor concentrations initialized at the circulating-fuel steady state. A +100 pcm step is imposed at t = 10 s. Because the thermal equations are solved for perturbations, reference heat generation and heat removal are implicitly balanced at t = 0; therefore, the 898 K reference does not represent an absolute isothermal state evolving toward thermal equilibrium.

The principal non-restricted model inputs are summarized here, while design-specific kinetic and

flow-residence parameters are omitted from the public manuscript. The effective delayed neutron fraction was 330pcm, and the fuel-temperature and density-feedback coefficients were −1.61pcm/K and −3.13 pcm/(kg·m³), respectively. The reflector heating fraction was 4.13% of the modeled power perturbation. The six regional RTC inputs [R1–R6] were [0.28, 0.28, 1.02, 1.02, 0.18, 0.18] pcm/K, which sum to 2.96 pcm/K. The previously reported static six-region RTC was +3.11 pcm/K [1], whereas the present transient model employs a region-wise coefficient set totaling +2.96 pcm/K based on the current OpenMC input set. Representative heat-transfer coefficients of 1500 and 1000 W/m²K were assumed at the fuel–reflector interface and outer heat-removal boundary, respectively.

2.1 Effective Delayed Neutron Fraction with Fuel Circulation

In a circulating-fuel MSR, delayed neutron precursors may decay outside of the active core, reducing their contribution to reactor kinetics. The effect of circulating fuel on the delayed neutron fraction was considered based on the spatial fission-source distribution obtained from OpenMC. The delayed neutron precursor (DNP) distribution was constructed from the tallied fission distribution over the reactor vessel and external flow path. The DNPs were transported along a one-dimensional axial channel from the lower to the upper core regions, and precursor decay was accounted for using the in-core and ex-core residence times for each delayed neutron group. The effective delayed neutron fraction used in the PKE model was then determined by considering the relative delayed neutron contribution available within the active core.

2.2 Reflector Heating and Thermal Model

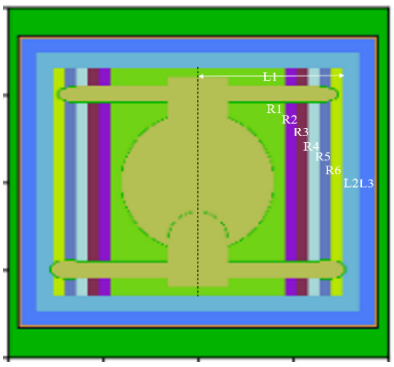


Fig. 2. Core and six-layer radial reflector assembly model.

Table I. Relative regional heating ratios obtained from OpenMC.

Region		Heating rate [%]
Active core		100
Clad		0.35
Reflector assembly	R1	3.07
	R2	0.42
	R3	0.23
	R4	0.17
	R5	0.13
	R6	0.11
	Total	4.13

As illustrated in Fig. 2, the reflector assembly was divided into six radial nodes to represent its spatially dependent thermal response. The neutronic geometry contains material-specific functional layers; in the present reduced-order thermal model, however, all six nodes are assigned equivalent BeO thermophysical properties to isolate the effects of spatial heating and RTC sensitivity. The OpenMC heating ratios are summarized in Table I.

Neutron and photon heating rates were tallied separately with OpenMC for each reflector layer. For the reduced-order transient model, these relative reflector-heating ratios were mapped to prescribed perturbation-power fractions, with the remaining power assigned to the fuel node. The listed clad heating was not modeled as an independent thermal node. The model accounts for conduction between neighboring reflector nodes and heat removal at the outer boundary. The model accounts for conduction between neighboring reflector nodes and heat removal at the outer boundary.

2.3 Region-wise Reflector Temperature Feedback

The reactivity sensitivity to reflector temperature was evaluated independently for each radial layer using OpenMC temperature perturbations around the reference condition. The calculated coefficients remained nearly constant over the investigated range, supporting a linear feedback approximation.

Accordingly, the transient reflector feedback was evaluated as

$$\rho_{\mathrm{RTC}}(t) = \sum_{i=1}^{6} \alpha_{\mathrm{RTC},i}\, \Delta T_{R,i}(t) \qquad (5)$$

where $\alpha_{\mathrm{RTC,i}}$ and $\Delta T_{\mathrm{R,i}}$ denote the RTC coefficient and temperature change of the i-th reflector layer, respectively.

2.4 Temperature-Dependent Properties and Coupling

Fuel-salt density was evaluated as a function of temperature using an ideal-liquid mixture model, and the resulting density change was incorporated explicitly as reactivity feedback. The BeO thermal-conductivity correlation was evaluated at 890 K, yielding 46.636 W/(m·K), and held constant during the transient; the reflector specific heat was set to 1350 J/(kg·K). Representative heat-removal parameters were prescribed at the outer reflector boundary.

At each time step, the PKE model determines reactor power, the prescribed heating fractions distribute the power perturbation to the fuel and reflector nodes,

and the thermal model updates ΔT_f and $\Delta T_{R,i}$. Fuel-temperature, fuel-density, and reflector-temperature feedbacks are then returned to the PKE model and solved with an implicit BDF time integrator. An instantaneous-RTC case, in which the equilibrium reflector feedback is applied without thermal delay, is used only as a no-delay reference.

3. Results

3.1 Spatial Dependence of Reflector Temperature Feedback

In our previous study[1], the temperature feedback characteristics of the BeO-reflected core were investigated using both single-region and spatially divided reflector models. The single-region treatment was found to overestimate neutron leakage during the uniform temperature perturbation, resulting in a less positive RTC than that obtained with the spatially resolved treatment. This finding motivated the use of a region-wise reflector model in the present transient analysis.

The single-region model yielded an RTC of approximately +2.89 pcm/K, whereas the six-region perturbation model yielded approximately +3.11 pcm/K, corresponding to an increase of about 7.6%. Based on the spatial dependence identified in the previous study, the six-region representation was adopted to evaluate the transient development of reflector temperature feedback.

The RTC remained approximately linear across the investigated temperature range, supporting the linear feedback approximation adopted in the transient model. A 100-pcm step reactivity insertion was then selected as a representative perturbation for comparing the temporal responses of the reflector models.

3.2 Spatial Thermal Response and RTC Contribution

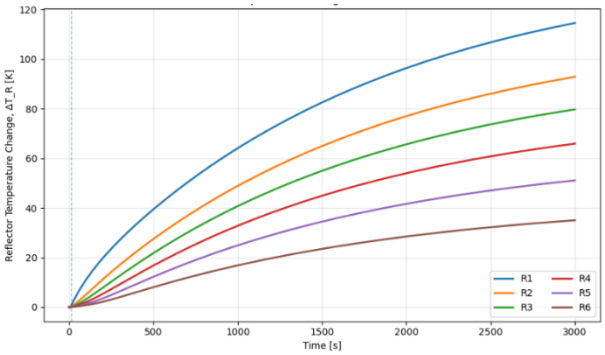


Fig. 3. Reflector temperature response by region.

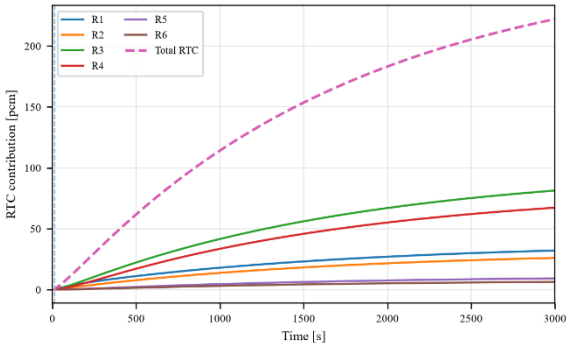


Fig. 4. Zone-wise RTC contribution.

The six-node thermal model predicted a non-uniform reflector temperature response. The innermost region adjacent to the core exhibited the largest temperature increase because of concentrated neutron/photon heating near the core–reflector interface and radial thermal resistance.

The zone-wise analysis showed that the positive RTC contribution depends on both local temperature rise and neutronic sensitivity. In the present input set, the largest long-term contributions arise from the high-sensitivity inner-to-middle reflector regions, demonstrating that heating, RTC sensitivity, and thermal transport must be considered together.

3.3 Transient Development of Positive RTC Effect

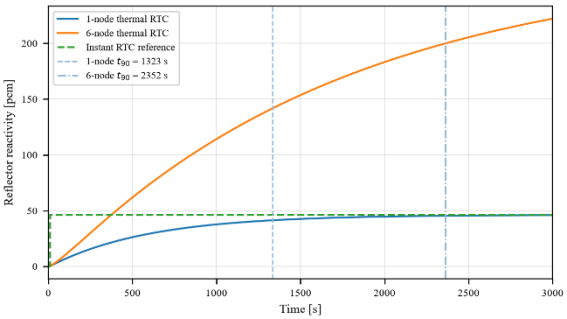


Fig. 5. RTC response: instant / 1-node / 6-node.

The spatially resolved model showed a slower development of the RTC than the one-node model. For the present input set, the one-node and six-node models reached 90% of their asymptotic RTC responses at approximately 1.32×10^3 s and 2.35×10^3 s, respectively.

The delayed response is mainly caused by the thermal inertia of the reflector assembly and radial thermal resistance between regions. Consequently, the positive RTC obtained from a static perturbation is not fully available immediately after the reactivity insertion; the negative fuel-temperature and fuel-density feedbacks develop earlier.

The one-node model asymptotically approaches the instantaneous-RTC reference because both are constructed to reproduce the same equilibrium feedback, while differing in whether reflector thermal delay is represented. The six-node model additionally resolves non-uniform heating, temperature response, and RTC

sensitivity, producing both a longer response time and a different equilibrium feedback magnitude.

The six-node model therefore predicts both a slower development and a larger long-term positive reflector feedback than the one-node representation. A static RTC alone is insufficient to characterize the transient response; the spatial sensitivity, heat deposition, and thermal transport time scale must be considered simultaneously.

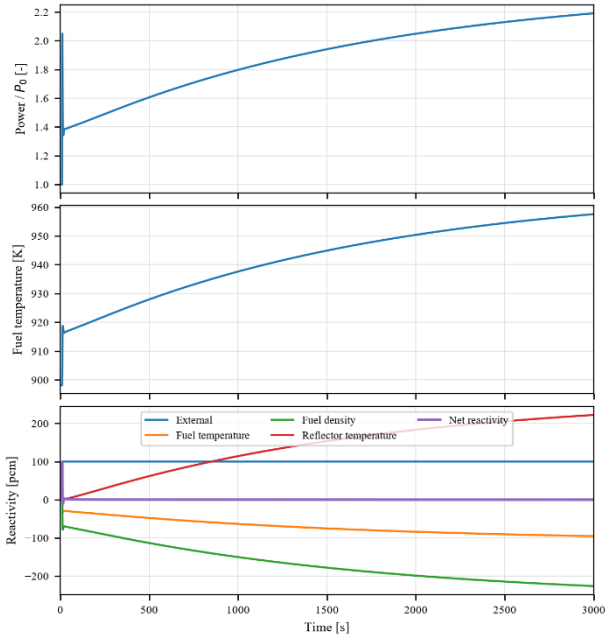


Fig. 6. Six-node multi-physics response: normalized power, fuel-salt temperature, and reactivity-feedback components.

Figure 6 shows the complete feedback balance for the coupled calculation. Following the +100 pcm insertion, power rises promptly, while fuel temperature and the associated negative fuel-temperature and density feedbacks respond before the slower positive reflector feedback. At 3000 s, the six-node calculation gives a fuel-temperature increase of about 59 K; the feedback components are approximately −95.6 pcm (fuel temperature), −226.4 pcm (density), and +222.0 pcm (RTC), leaving the total thermal feedback close to −100 pcm. Together with the +100 pcm external insertion, the net incremental reactivity therefore approaches zero as the system evolves toward a quasi-equilibrium state.

4. Conclusions

This study investigated the spatial and temporal characteristics of positive reflector temperature feedback in a BeO-reflected fast-spectrum MSR using a perturbation-form PKE–1D thermal model. The spatially resolved representation predicted a slower and larger positive RTC response than the one-node model, and the multi-physics results confirmed that negative fuel-temperature and density feedbacks act before the full positive reflector feedback develops.

The delayed emergence of the positive RTC is favorable to the early transient reactivity balance, but the increasing positive reflector feedback offsets part of the negative fuel feedback at longer times. Reflector design and transient safety assessment should therefore consider both RTC magnitude and response time.

The present model solves temperature perturbations about a prescribed reference state; therefore, the uniform 898 K reference does not represent an absolute isothermal heat-up calculation. Future work will extend the model to an absolute-temperature formulation initialized from a converged OpenMC–thermal-hydraulic steady-state temperature distribution, so that the effect of an external reactivity insertion can be evaluated from a realistic pre-existing reflector temperature gradient. Broader design studies will then examine reflector material, thickness, cooling, peak power, maximum fuel temperature, and settling time, followed by higher-fidelity three-dimensional heat-transfer and spatial-kinetics verification.

ACKNOWLEDGMENTS

This work was supported by a grant from the Korea Research Institute for Defense Technology Planning and Advancement (KRIT), funded by the Korean government through the Defense Acquisition Program Administration (DAPA) (KRIT-CT-22-017, Next Generation Multi-Purpose High Power Generation Technology [Liquid-Fueled Heat Supply Module Design Technology], 2022).

REFERENCES

[1] S. J. Yoon, J. U. Seo, S. K. Zee, T. K. Park, and S. J. Kim, “Decomposition of Reactor Temperature Coefficients with Spatially Heterogeneous Reflector Temperature Effects in Molten Salt Reactors,” Transactions of the Korean Nuclear Society Spring Meeting, Jeju, Korea, 2026.

[2] Y. J. Lee, E. Lee, J. H. Kim, and Y. Kim, “Reflector Temperature Coefficient of Molten Salt Fast Reactor Using Moderating Reflector,” Progress in Nuclear Energy, vol. 191, 106091, 2026.

[3] J. J. Jeong and Y. Cho, “Analytical Derivation of Steady-State Delayed Neutron Precursor Distribution and Effective Delayed Neutron Fraction in a Molten Salt Reactor,” Nuclear Engineering and Technology, vol. 58, no. 5, 104160, 2026.

[4] W. Park and Y. H. Jeong, “Systematic Investigation on Neutronics and Thermal-Hydraulics Model for Multi-Physics Analysis of Micro Molten Salt Fast Reactor with Moderating Reflector,” Nuclear Engineering and Technology, vol. 58, no. 5, 104114, 2026.

[5] D. A. Andersson, G. Wang, P. Yang, and B. W. Beeler, “KCl-UCl_3 Molten Salts Investigated by Ab Initio Molecular Dynamics (AIMD) Simulations: A Comparative Study with Three Dispersion Models,” Journal of Nuclear Materials, vol. 599, 155226, 2024.

[6] M. D. Hou, X. W. Zhou, and B. Liu, “Beryllium Oxide Utilized in Nuclear Reactors: Part I: Application History, Thermal Properties, Mechanical Properties, Corrosion Behavior and Fabrication Methods,” Nuclear Engineering and Technology, vol. 54, no. 12, pp. 4393–4411, 2022.